Separation Science and Technology
Publication details, including instructions for authors and subscription information:
http://www.informaworld.com/smpp/title~content=t713708471

Phosphate Removal from Aqueous Solution Using Coir-Pith Activated Carbon

Pradeep Kumar[ab]; S. Sudha[a]; Shri Chand[a]; Vimal Chandra Srivastava[a]
[a] Department of Chemical Engineering, Indian Institute of Technology Roorkee, Roorkee, Uttarakhand, India [b] Department of Chemical Engineering and Technology, Institute of Technology, Banaras Hindu Univeristy, Varanasi, Uttar Pradesh, India

To cite this Article Kumar, Pradeep , Sudha, S. , Chand, Shri and Srivastava, Vimal Chandra(2010) 'Phosphate Removal from Aqueous Solution Using Coir-Pith Activated Carbon', Separation Science and Technology, 45: 10, 1463 — 1470
To link to this Article: DOI: 10.1080/01496395.2010.485604
URL: http://dx.doi.org/10.1080/01496395.2010.485604

Separation Science and Technology, 45: 1463–1470, 2010

ISSN: 0149-6395 print/1520-5754 online
DOI: 10.1080/01496395.2010.485604

Taylor & Francis
Taylor & Francis Group

Phosphate Removal from Aqueous Solution Using Coir-Pith Activated Carbon

Pradeep Kumar,[1,2] S. Sudha,[1] Shri Chand,[1] and Vimal Chandra Srivastava[1]
[1]*Department of Chemical Engineering, Indian Institute of Technology Roorkee, Roorkee, Uttarakhand, India*
[2]*Department of Chemical Engineering and Technology, Institute of Technology, Banaras Hindu Univeristy, Varanasi, Uttar Pradesh, India*

The present study deals with the removal of phosphates from aqueous solution using activated carbon developed from coir pith. Batch adsorption experiments were performed to delineate the effect of initial pH, contact time, adsorbent dose and temperature on the removal of phosphates by coir-pith activated carbon (CAC) (activated by H_2SO_4). The removal was found to be maximum in the pH range of 6–10. The kinetics of adsorption showed that the phosphate adsorption onto CAC was a gradual process with a quasi-equilibrium being attained in 3 h. The adsorption equilibrium data followed the Temkin isotherm. Thermodynamic parameters such as ΔG^o, ΔH^o, and ΔS^o were evaluated by applying the Arrhenius and van't Hoff equations, and it was found that the adsorption of phosphate on CAC was spontaneous and endothermic.

Keywords adsorption; adsorption kinetics; coir pith activated carbon; phosphate; thermodynamics

INTRODUCTION

Phosphates (P) discharged into water bodies like lakes, ponds, rivers, etc. act as a major nutrient for the aquatic life leading to overgrowth of algae (eutrophication). This affects the water quality through consumption of dissolved oxygen and destroys aquatic life (1). In the past few decades, usages of both synthetic and animal-based fertilizers have caused discharge of excess P as a non-point-source agricultural pollutant throughout the world (2). Ps are also released from the detergents and pigment formulation, and mineral processing industries (3–4). Typically raw domestic wastewater has a total P concentration of approximately 10 mg/l, the principal forms of P being orthophosphate (5 mg/l), pyrophosphate (1 mg/l), and tripolyphosphate (3 mg/l), together with smaller amounts of organic phosphates (5). Removal of P from wastewater is, therefore, necessary to meet the discharge limit to control the pollution. The Indian discharge limits for phosphate (PO_4^{3-}) as P is 5.0 mg/l (6). Removal of PO_4^{3-} is, therefore, reported as an equivalent amount of P. To meet the effluent quality standards, the removal of P from wastewaters prior to discharge into natural waters is required.

Various techniques like physico-chemical and biological methods have been successfully used for the removal of P (7). Chemical precipitation with lime, alum, and iron salts is effective for P removal; however, there are problems of sludge handling, its disposal, and neutralization of the effluent. Various investigators have studied the adsorptive removal of P from aqueous solution using various adsorbents such as calcium silicate (8), tamarind nut shell activated carbon (9), iron oxide tailings (10), dolomite (11), fly ash (12), Fe(III)/Cr(III) hydroxides (13), aluminum oxide hydroxide (14), activated red mud (15), goethite (16), ferromanganese nodules (17), calcined MgMn-layered double hydroxides (18), and activated alumina (19).

Coir pith is generated in the process of separation of the fiber from coconut husk. India, the third largest producer of coconuts in the world, produces about 12.8 billion coconuts a year (3). It is estimated that the production of coir pith in India is about 0.5 million tons per year (4). Accumulation of coir pith around coir industries is a big menace, since it is not easily biodegradable. Preparation of activated carbons from this cheap and abundant biomass will not only eliminate the problem of coir-pith disposal but it will derive economic benefits from such value-added products.

The objective of the present study was to evaluate the potential of coir-pith activated carbon (CAC) (activated by H_2SO_4) for the removal of phosphates from aqueous solution.

EXPERIMENTAL PROCEDURE

Adsorbent

Coir pith, collected from a nearby coir industry, was washed with the distilled water and dried in sunlight. The dried material was washed with 98% sulfuric acid, with

---

Received 26 November 2008; accepted 5 April 2010.

Address correspondence to Shri Chand, Department of Chemical Engineering, Indian Institute of Technology Roorkee, Roorkee 247667, Uttarakhand, India. Tel.: +91-1332-285383 (O); Fax: +91-1332-276535, 273560. E-mail: schanfch@iitr.ernet.in

the weight ratio being 1 part of coir pith to 1.8 parts of acid, and kept at room temperature for about 5 h with occasional stirring. The acid-carbonized coir pith was washed several times with distilled water and with 5% sodium bicarbonate solution, followed by distilled water for the removal of the remaining amount of acid. The dried coir-pith was carbonized in a muffle furnace at 600°C for 1 h in absence of air flow (20).

The physico-chemical characterization of CAC was performed. A proximate analysis carried out using the standard procedure showed 18.8% moisture, 20.9% volatile matter, 3.2% ash, and 57.1% fixed carbon. Bulk density was determined using MAC bulk density meter. A high amount of carbon indicates that CAC is basically organic in nature and was found to be 318.9 kg/m^3. For morphological characterization, scanning electron micrograph (SEM) analyses were carried out. The Brunauer–Emmett–Teller (BET) surface area and the BET average pore size of CAC were found to be 727.4 m^2/g and 18.79 Å, respectively. The point of zero charge (pH_{PZC}) of CAC was found to be 9.9.

Adsorbate

All reagents used in this study were of analytical reagent (AR) grade. A 1 g/l P stock solution was prepared dissolving an accurate quantity of potassium dihydrogen phosphate salt (KH_2PO_4). All experimental solutions of P were prepared by proper dilution of this stock solution with distilled water. The initial pH (pH_o) of the solution was adjusted to the desired value using 0.1 M NaOH or 0.1 M H_2SO_4 solution prior to addition of adsorbent.

Batch Adsorption Studies

Adsorption experiments were carried out by agitating 100 ml of P solution of known initial concentration (C_0), pH_0 and a known amount of the CAC in a 250 ml stoppered conical flask. This mixture was agitated in a temperature-controlled shaking water bath at a constant speed at 35 ± 1°C. Samples were withdrawn at appropriate time intervals. Concentration of P in the supernatant was estimated with UV-visual spectrophotometer by stannous chloride method, monitoring the absorbance at 690 nm (21). The effect of pH_0 on P removal was studied over a pH_0 range of 2 to 11. For the optimum amount of adsorbent dose, 100 ml P solution was contacted with different amounts of CAC till equilibrium was attained. The kinetics of adsorption was determined by analyzing the adsorptive uptake of the P from the aqueous solution at different time intervals. For adsorption isotherms, P solutions of different concentrations were agitated with the known amount of CAC till equilibrium was achieved. The residual P concentration of the solution was then determined. To see the effect of temperature on the adsorption of P from solution by CAC, experiments were also conducted at 35, 50, and 60°C. For desorption study, P-loaded CAC (0.1 g) was agitated at 150 rpm in a series of 250 ml conical flasks containing 50 ml of aqueous solution (0.1 N) of HNO_3, acetone and distilled water at 303 K for 24 h in the orbital shaker.

RESULTS AND DISCUSSION

Effect of Initial pH (pH_0)

Figure 1 shows the effect of pH_0 on the removal of P by CAC. For $pH_0 < 6$ and $pH_0 > 10$ the removal is lower, and for $6 < pH_0 < 10$ removal of P is maximum and nearly constant. Depending on the pH of the system, P exists as H_3PO_4, $H_2PO_4^-$, HPO_4^{2-}, and PO_4^{3-}. At pH 2, the P exists predominantly as H_3PO_4. This neutral species is weakly attached to the sites of the adsorbent. The pH_{PZC} of CAC was found to be 9.9. For $6 < pH_0 < 10$, prevalent species of P such as $H_2PO_4^-$ and HPO_4^{2-} are anionic in nature, and are easily adsorbed onto the positive surface of CAC. At $pH_0 > 10$, the concentration of OH^- in solution becomes high and competes with the PO_4^{-3} species for the adsorption sites resulting in decrease of P removal. Also, at higher pH, the negatively charged CAC surface does not favor the adsorption of anion due to the electrostatic repulsion. The final pH values (pH_f) of the sorption process are shown as a function of pH_0 in Fig. 1. The pH_f values are higher than the pH_0 values for pH < 10, excepting for some experiments with higher pH_0 (>10). Though the P removal by CAC sharply increased with increasing pH_0, however, the pH_f values were more or less constant for the pH_0 values in the range of 8–12. These pH_f values are, therefore, considered to indicate the equilibrium pH values.

SEM of CAC (Fig. 2) were taken before and after adsorption. This photomicrograph shows the fibrous structure of CAC. However, the surface of the CAC becomes smooth after adsorption of P due to the coverage of pores. Figure 3

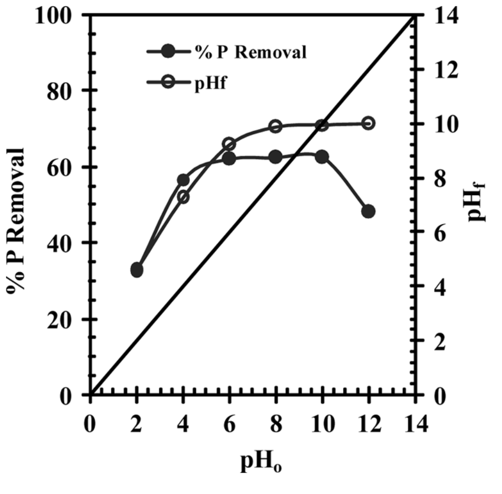

FIG. 1. Effect of pH$_o$ on the adsorption of phosphate using coir-pith activated carbon as adsorbent. T = 308 K, t = 3 h, C_0 = 20 mg/l, Coir-pith activated carbon dose = 4 g/l.

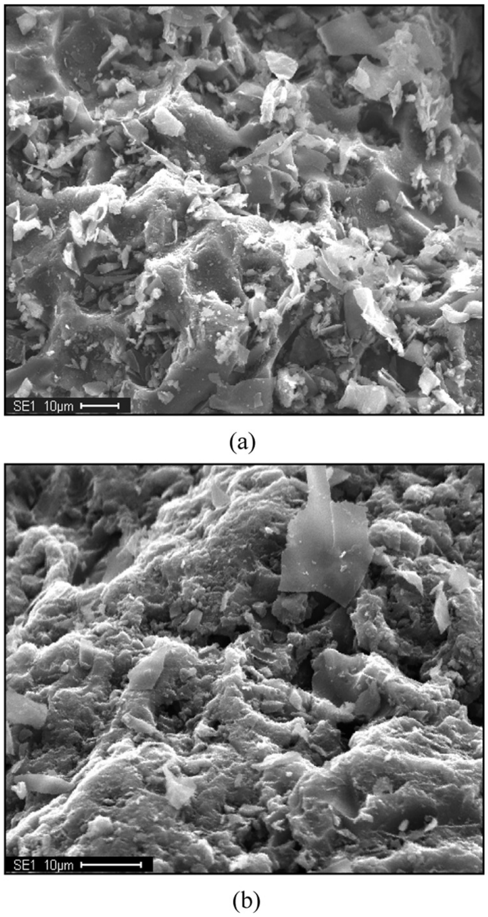

FIG. 2. Scanning electron micrograph of coir-pith activated carbon (a) before, and (b) after phosphate adsorption from aqueous solution.

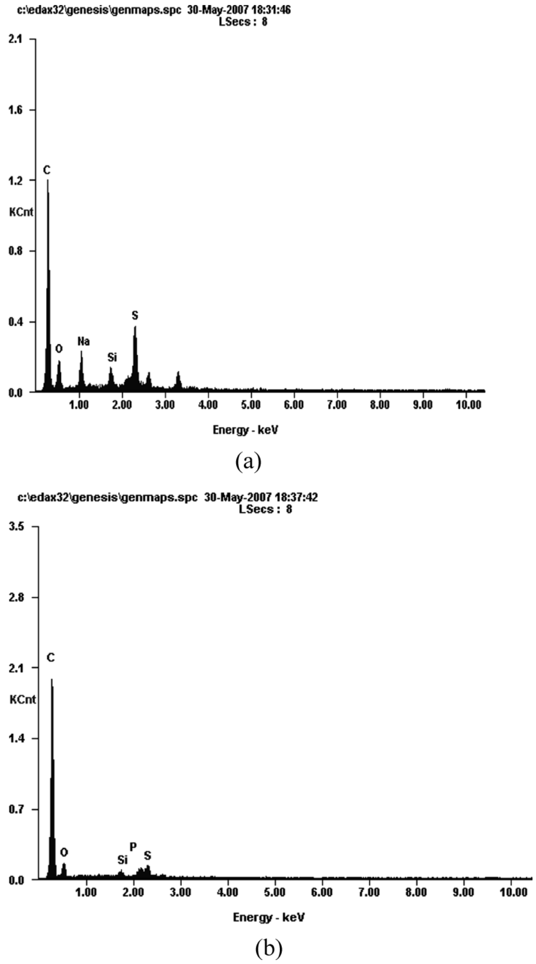

FIG. 3. Energy dispersive spectrum of coir-pith activated carbon (a) before, and (b) after phosphate adsorption from aqueous solution.

shows the energy dispersive spectrum (EDS) of CAC before and after adsorption. Figure 3a reveals that the CAC contains high carbon besides silica, sodium, sulphur, etc. In addition to these elements, P is also found in Figure 3b due to the adsorption of P onto CAC.

Effect of Adsorbent Dosage

The effect of dose on the removal of P by CAC at initial concentration $C_0 = 20$ mg/l is shown in Fig. 4. It can be seen that the P removal increases up to a certain limit and then it remains almost constant. Optimum dose was found to be 4 g/l. The percent removal increased with increase in the adsorbent dose due to a higher mass (total surface area) of the adsorbent particles.

Effect of Agitation Time (T) and Initial Phosphate Concentration (C_0)

The effects of t and C_0 on the removal of P by CAC are shown in Fig. 5. It is evident that the amount of P adsorbed per unit mass of adsorbent (q_t) increased with C_0 and remained constant after equilibrium time. q_t increases with the increase in C_0 as the resistance to the uptake of P from the solution decreases with the increase in C_0. The rate of adsorption also increases with the increase in C_0 due to increase in the driving force. The equilibrium time is found to be 60 min for C_0 value of 10 mg/l, 120 min for 20 mg/l, and 180 min for 40 mg/l.

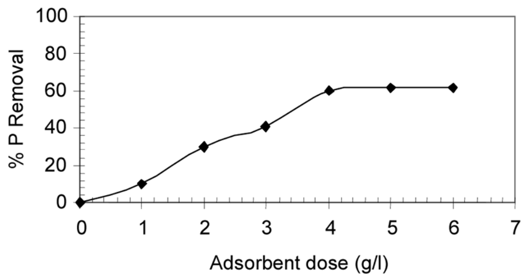

FIG. 4. Effect of adsorbent dose on the adsorption of phosphate using coir-pith activated carbon as adsorbent. T = 308 K, $t = 3$ h, $C_0 = 20$ mg/l, pH = 6.

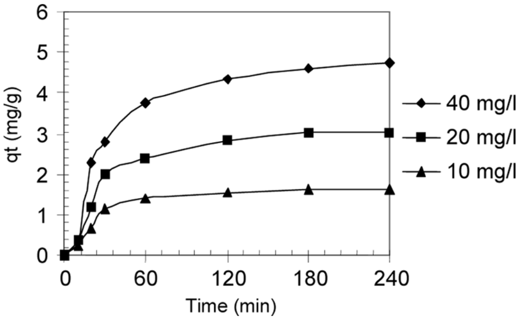

FIG. 5. Effect of agitation time and concentration of phosphate on amount adsorbed using coir-pith activated carbon as adsorbent. T = 308 K, $t = 4$ h, pH = 6, Coir-pith activated carbon dose = 4 g/l.

Adsorption Kinetics Study

The pseudo-first-order (22) and the pseudo-second-order kinetic models (23) are given by Eqs. (1) and (2)

$$q_t = q_e\left\lfloor 1 - \exp(-k_f t)\right\rfloor \qquad (1)$$

$$q_t = \frac{tk_S q_e^2}{1 + tk_S q_e} \qquad (2)$$

where, q_t is the amount of adsorbate adsorbed at time t (mg/g), q_e is the adsorption capacity at equilibrium (mg/g), k_f is the pseudo-first-order rate constant (min^{-1}), k_S is the pseudo-second-order rate constant (g/mg/min) and t is the contact time (min).

The values of adsorption rate constant (k_f) for P adsorption on CAC at $C_0 = 10$, 20, and 40 mg/l were determined using non-linear regression, and are given in Table 1. The calculated correlation coefficients are closer to unity, and also $q_{e,calc}$ are better predicted by the pseudo-first-order kinetic model. Therefore, the adsorption can be approximated more appropriately by the pseudo-first-order kinetic model. Similarly, the pseudo-first-order kinetic model has been found to better represent the adsorption kinetics of P onto alunite (24); fly ash, slag, ordinary Portland cement, and related blends (25).

Intra-Particle Diffusion Study

The transport of the adsorbate from the solution phase to the surface of the adsorbent particles may be controlled either by one or more steps, e.g., film or external diffusion, pore diffusion, surface diffusion and

TABLE 1

Kinetic parameters for the removal of phosphates from waste water by coir-pith activated carbon. $pH_0 = 6$, $T = 308$ K, $C_0 = 10$, 20, and 40 mg/l, CAC dose = 4 g/l

C_o (mg/l)	$q_{e,\,\mathrm{exp}}$ (mg/g)	$q_{e,\,cal}$ (mg/g)	k_f (1/min)	R^2
		Pseudo-first-order		
10	1.618	1.3605	0.0251	0.9593
20	3.028	2.6375	0.0219	0.9587
40	4.755	3.8054	0.0182	0.9768

C_o (mg/l)	$q_{e,\,\mathrm{exp}}$ (mg/g)	$q_{e,\,cal}$ (mg/g)	k_S (g/mg min)	R^2
		Pseudo-second-order		
10	1.618	1.9588	0.0127	0.9436
20	3.028	3.8095	0.0053	0.9434
40	4.755	6.4474	0.0022	0.8092

C_o (mg/l)	k_{id1} (mg/g min$^{1/2}$)	I (mg/g)	R^2
	Intra-particle diffusion		
10	0.3961	1.0496	0.9865
20	0.6972	1.8645	0.9946
40	1.0707	2.8522	0.9424

C_o (mg/l)	k_{id2} (mg/g min$^{1/2}$)	I (mg/g)	R^2
	Intra-particle diffusion		
10	0.0313	1.1677	0.9017
20	0.0835	1.8258	0.9017
40	0.1308	2.8006	0.9636

adsorption on the pore surface, or a combination of more than one step. Generally, a process is diffusion controlled if its rate is dependent upon the rate at which components diffuse towards one another. The possibility of intra-particle diffusion was explored by using the Weber-Morris diffusion model (26).

$$q_t = k_{id}t^{0.5} + I \tag{3}$$

where, k_{id} is the intra-particle diffusion rate constant (mg/g min$^{0.5}$) and I (mg/g) is a constant that gives an idea about the thickness of the boundary layer, i.e., the larger the value of I the greater is the boundary layer effect (27). If the Weber-Morris plot of q_t versus $t^{0.5}$ satisfies the linear relationship with the experimental data, then the adsorption process is found to be controlled by intra-particle diffusion only. However, if the data exhibit multi-linear plots, then two or more steps influence the adsorption process.

In the q_t versus $t^{0.5}$ plot (Fig. 6) the data points are related by two straight lines—the first straight portion depicting macro pore diffusion and the second representing meso pore diffusion. These show only the pore diffusion data. The deviation of straight lines from the origin (Fig. 6) may be due to a difference in the rate of mass transfer in the initial and final stages of adsorption. Further, such deviation of a straight line from the origin indicates that the pore diffusion is not the sole rate-controlling step. The initial curvature in the adsorption data for q_t versus $t^{0.5}$ is attributed to boundary layer diffusion effects. The values of rate parameters ($k_{id,1}$ and $k_{id,2}$) are given in Table 1.

Effect of Temperature

Figure 7 shows the plots of q_t versus t for P-CAC system at 308, 323 and 333 K. It shows that the increase in temperature slightly increased the amount adsorbed (mg/g). Figure 7 shows that the increase in P removal with an increase in temperature from 308–333 K is more significant in the first 30 min only and the effect diminishes with progress in time. The increase in uptake of P with temperature may be due to the desolvation of the adsorbing species and the enhanced rate of intra-particle diffusion of adsorbate, as diffusion is an endothermic process.

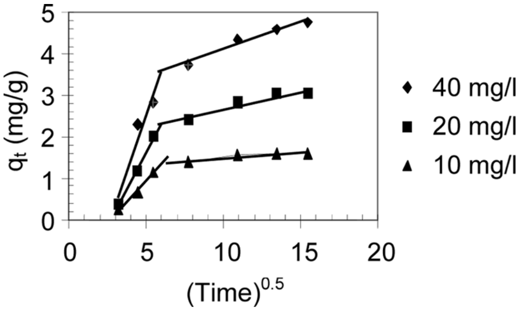

FIG. 6. Weber and Morris intra-particle diffusion plot for the removal of phosphate using coir-pith activated carbon as adsorbent. T = 308 K, coir-pith activated carbon dose = 4 g/l, pH = 6, t = 3 h.

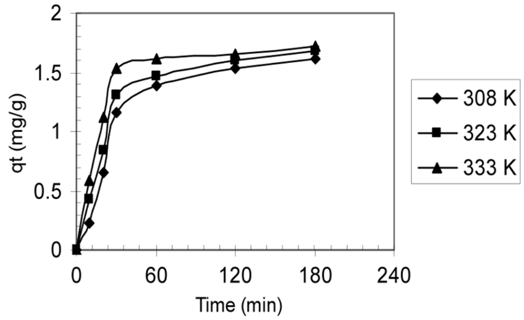

FIG. 7. Effect of temperature on removal of phosphate by using coir-pith activated carbon as adsorbent. t = 3 h, pH = 6, coir-pith activated carbon dose = 4 g/l, C_0 = 10 mg/l.

Adsorption Isotherms

To establish the most appropriate correlation for representing the equilibrium curves, Langmuir, Freundlich, and Temkin isotherms given by Eqs. (4) to (6), respectively, were tested. The details of these isotherms are well known (28).

$$q_e = \frac{q_m K_L C_e}{1 + K_L C_e} \tag{4}$$

$$q_e = K_F C_e^{1/n} \tag{5}$$

$$q_e = B_1 \ln(K_T C_e) \tag{6}$$

where, q_e is the fraction of the adsorbate on the under equilibrium condition (mg/g), C_e the equilibrium metal ion concentration (mg/l), K_L the Langmuir adsorption constant (l/mg) related to the energy of adsorption, and q_m the adsorption capacity of the adsorbent (mg/g). K_F is the Freundlich constant (l/mg), and $(1/n)$ the heterogeneity factor, K_T is the equilibrium binding constant (l/mg) corresponding to the maximum binding energy and constant B_1 is related to the heat of adsorption.

The Marquardt's percent standard deviation (MPSD) error function (29) was used to test the adequacy of the isotherm equations to represent the experimental data. This error function is given as

$$MPSD = 100\sqrt{\frac{1}{n-p}\sum_{i=1}^{n}\left(\frac{(q_{e,meas} - q_{e,calc})}{q_{e,meas}}\right)_i^2} \tag{7}$$

The parameters of the isotherms and the correlation coefficient, R^2, as determined by using the solver add-in

TABLE 2

Isotherm parameters for removal of phosphates from aqueous solution by coir-pith activated carbon. $pH_0 = 6$, $t = 3$h, CAC dose $= 4$ g/l

T (K)	K_F ((mg/g)/(mg/l)$^{1/n}$)	$1/n$	R^2	MPSD
		Freundlich constants		
308	0.7888	0.6122	0.9887	11.7924
323	0.9060	0.5641	0.9869	11.7664
333	1.1806	0.2998	0.9929	52.3667

T (K)	K_L (l/mg)	Q$_m$ (mg/g)	R_L	R^2	MPSD
		Langmuir constants			
308	0.0782	7.7399	0.3731	0.9980	4.4255
323	0.0951	7.2622	0.3551	0.9986	4.1763
333	0.0956	7.5586	0.3539	0.9998	0.6207

T (K)	K_T (l/mg)	B_1	R^2	MPSD
		Temkin constants		
308	0.7055	1.7747	0.9999	0.8723
323	0.8284	1.6912	0.9999	1.1868
333	0.8513	1.74	0.9995	2.6062

function of the MS excel, for the fitting of the experimental data are listed in Table 2. By comparing the results of the values for the MPSD error function and the correlation coefficients, it is found that the Temkin isotherm best represents the equilibrium adsorption of P by CAC.

Thermodynamic Study

The Gibbs-free energy change of the adsorption process is related to the equilibrium constant by the classic Van't Hoff equation

$$\Delta G^0 = -RT \ln K_D \tag{8}$$

According to thermodynamics, the Gibbs free energy change is also related to the entropy change and heat of adsorption at constant temperature by the following equation:

$$\Delta G^0 = \Delta H^0 - T\Delta S^0 \tag{9}$$

Combining the above two equations, we get

$$\ln K_D = \frac{-\Delta G^0}{RT} = \frac{\Delta S^0}{R} - \frac{\Delta H^0}{R}\frac{1}{T} \tag{10}$$

where, ΔG^0 is the free energy change (kJ/mol), ΔH^0 is the change in enthalpy (kJ/mol), ΔS^0 is the entropy change (J/mol K), T is the absolute temperature (K), R is the universal gas constant (8.314 J/mol K), and K_D is the thermodynamic equilibrium constant. K_D for the adsorption reaction can be defined:

$$K_D = \frac{a_s}{a_e} = \frac{\nu_s}{\nu_e}\frac{C_o}{C_e} \tag{11}$$

where, a_s is the activity of the adsorbed solute, a_e the activity of the solute in the equilibrium solution, ν_s is the activity coefficient of the adsorbed solute, and ν_e the activity coefficient of the solute in the equilibrium solution. As the concentration of the solute in the solution approaches zero, the activity coefficient ν approaches unity. Equation (11) may then be written as:

$$\lim_{Ce\to 0}\frac{C_o}{C_e} = \frac{a_s}{a_e} = K_D \tag{12}$$

Values of K_D are obtained by plotting ln (C_o/C_e,) versus C_e, and extrapolating to zero C_e (30). The increase in K_D with increase in temperature indicates the endothermic nature of the process. ΔH^0 and ΔS^0 are determined from the slope and intercept of the linear plot of ln K_D vs $1/T$. The thermodynamic parameters for the P adsorption onto CAC are given in Table 3. The positive ΔH^0 value confirms the endothermic nature of the overall-adsorption process. The adsorption process in the solid-liquid system is a combination of two processes:

(a) the desorption of the molecules of solvent (water) previously adsorbed and
(b) the adsorption of adsorbate species.

TABLE 3
Thermodynamic parameters for adsorption of phosphates by coir-pith activated carbon

T (K)	K_D	$-\Delta G^0$ (kJ/mol K)	ΔH^0 (kJ/mol)	ΔS^0 (J/kmol)
308	3.0502	2.856	3.8843	21.8849
323	3.2766	3.187		
333	3.4175	3.402		

The valve of ΔH^0 is less than 20 kJ/mol indicating physical nature of the adsorption process.

In the desorption study, HNO_3 and acetone showed desorption efficiencies of 70.1% and 61.4%, respectively. Water showed the desorption efficiency of 19.2% only. Higher desorption efficiency by HNO_3 and acetone could be attributed to the physical nature of attachment between CAC and adsorbed P. However, negligible desorption by water shows the presence of some chemical attachment between the adsorbate and the adsorbent.

The positive value of ΔS^0 suggests increased randomness at the solid/solution interface with some structural changes in the adsorbate and adsorbent, and an affinity of the P towards CAC. Also, the positive ΔS value corresponds to decrease in the degree of freedom of the adsorbed species (28).

CONCLUSIONS

This study shows that the H_2SO_4-treated activated carbon developed from the agricultural waste coir-pith is an effective and low-cost adsorbent for the removal of phosphates (P) from waste water. The percentage removal of P was found to be maximum in the pH range of 6 to 10. The optimum adsorbent dose was 4 g/l of solution. The experimental data predict that the pore diffusion is not the sole rate-controlling step. Adsorption kinetics obeyed a first-order kinetic model. An increase in temperature slightly increased the removal of P by CAC. Temkin isotherm was found to represent the adsorption equilibrium data well. The negative values of ΔG^0 indicates that the adsorption of P onto CAC is feasible and spontaneous. ΔH^0 and ΔS^0 were found to be 3.88 kJ/mol and 21.88 J/K mol, respectively.

ACKNOWLEDGEMENTS

One of the authors, SS, is thankful to the Ministry of Human Resource Development (MHRD), Government of India for providing financial assistance for carrying out this research work.

REFERENCES

1. Bektas, N.; Akbulut, H.; Inan, H.; Dimoglo, A. (2004) Removal of phosphate from aqueous solutions by electro-coagulation. *J. Hazard. Mater.*, 106B: 101–105.
2. Arai1, Y.; Sparks, D.L. (2001) ATR–FTIR spectroscopic investigation on phosphate adsorption mechanisms at the ferrihydrite–water interface. *J. Colloid Interf. Sci.*, 241: 317–326.
3. Huynh, L.; Jenkins, P. (2001) A rheological and electrokinetic investigation of the interactions between pigment particles dispersed in aqueous solutions of short-chain phosphates. *Colloid Surface A: Physicochem. Eng. Aspects*, 190: 35–45.
4. Gao, Y.; Mucci, A. (2001) Acid base reactions, phosphate and arsenate complexation, and their competitive adsorption at the surface of goethite in 0.7 M NaCl solution. *Geochimica et Cosmochimica Acta*, 65: 2361–2378.
5. Eilbeck, W.J.; Mattock, G. (1981) *Chemical Processes in Wastewater Treatment*; Wiley: New York, 271–276.
6. Central Pollution Control Board, Ministry of Environment and Forests, Govt. of India, Delhi, http://www.cpcb.nic.in/standard welcome.htm.
7. Yeoman, S.; Stephenson, T.; Lester, J.N.; Perry, R. (1988) The removal of phosphorus during wastewater treatment, A review. *Environ. Pollut.*, 49: 183–233.
8. Southam, D.C.; Lewis, T.W.; McFarlane, A.J.; Johnston, J.H. (2004) Amorphous calcium silicate as a chemisorbent for phosphate. *Curr. Appl. Phys.*, 4: 355–358.
9. Bhargava, D.S.; Sheldarkar, S.B. (1993) Use of TNSAC in phosphate adsorption studies and isotherm relationships and utility in the field. *Water Res.*, 27 (2): 325–335.
10. Zeng, L.; Li, X.; Liu, J. (2004) Adsorptive removal of phosphate from aqueous solutions using iron oxide tailings. *Water Res.*, 38: 1318–1326.
11. Karaca, S.; Gurses, A.; Ejder, M.; Acikyildiz, M. (2004) Kinetic modeling of liquid-phase adsorption of phosphate on dolomite. *J. Colloid Interf. Sci.*, 277: 257–263.
12. Oguz, E. (2005) Sorption of phosphate from solid/liquid interface by fly ash. *Colloid Surface A: Physicochem. Eng. Aspects*, 262: 113–117.
13. Namasivayam, C.; Prathap, K. (2005) Recycling Fe(III)/Cr(III) hydroxide, an industrial solid waste for the removal of phosphate from water. *J. Hazard. Mater.*, B123: 127–134.
14. Tanada, S.; Kabayama, M.; Kawasaki, N.; Sakiyama, T.; Nakamura, T.; Araki, M.; Tamura, T. (2003) Removal of phosphate by aluminum oxide hydroxide. *J. Colloid Interf. Sci.*, 257: 135–140.
15. Pradhan, J.; Das, J.; Das, S.; Thakur, R.S. (1998) Adsorption of phosphate from aqueous solution using activated red mud. *J. Colloid Interf. Sci.*, 204: 169–172.
16. Wang, K.; Xing, B. (2004) Mutual effects of cadmium and phosphate on their adsorption and desorption by goethite. *Environ. Pollut.*, 127: 13–20.
17. Parida, K.M.; Mohanty, S. (1998) Studies on Indian Ocean manganese nodules. Part VIII. Adsorption of aqueous phosphate on ferromanganese nodules. *J. Colloid Interf. Sci.*, 199: 22–27.
18. Chitrakar, R.; Tezuka, S.; Sonoda, A.; Sakane, K.; Ooi, K.; Hirotsu, T. (2005) Adsorption of phosphate from seawater on calcined MgMn-layered double hydroxides. *J. Colloid Interf. Sci.*, 290: 45–51.
19. Hano, T.; Takanashi, H.; Hirata, M.; Urano, K.; Eto, S. (1997) Removal of phosphorus from wastewater by activated alumina adsorbent. *Water Sci. Technol.*, 35: 39–46.
20. Sekar, M.; Sakthi, V.; Rengaraj, S. (2004) Kinetics and equilibrium adsorption study of lead (II) onto activated carbon prepared from coconut shell. *J. Colloid Interf. Sci.*, 279: 307–313.
21. APHA. (1980) *Standard Methods for the Examination of Water and Wastewater*, 15th Ed.; American Public Health Association: Washington, DC, 368–369.

22. Srivastava, V.C.; Mall, I.D.; Mishra, I.M. (2006) Characterization of mesoporous rice husk ash (RHA) and adsorption kinetics of metal ions from aqueous solution onto RHA. *J. Hazard. Mater.*, B134: 257–267.
23. Ho, Y.S.; McKay, G. (1999) Pseudo-second order model for sorption processes. *Process Biochem.*, 34: 451–465.
24. Ozacar, M. (2003) Adsorption of phosphate from aqueous solution onto alunite. *Chemosphere*, 51: 321–327.
25. Agyeia, N.M.; Strydom, C.A.; Potgieter, J.H. (2002) The removal of phosphate ions from aqueous solution by fly ash, slag, ordinary Portland cement and related blends. *Cement Concrete Res.*, 32: 1889–1897.
26. Weber, Jr. W.J.; Morris, J.C. (1963) Kinetics of adsorption on carbon from solution. *J. Sanitary Engg. Div. ASCE*, 89 (SA2): 31–59.
27. Kannan, K.; Sundaram, M.M. (2001) Kinetics and mechanism of removal of methylene blue by adsorption on various carbons – a comparative study. *Dyes Pigment*, 51: 25–40.
28. Srivastava, V.C.; Mall, I.D.; Mishra, I.M. (2007) Adsorption thermodynamics and isosteric heat of adsorption of toxic metal ions onto bagasse fly ash (BFA) and rice husk ash (RHA). *Chem. Eng. J.*, 132: 267–278.
29. Marquardt, D.W. (1963) An algorithm for least-squares estimation of nonlinear parameters. *J. Soc. Ind. Appl. Math.*, 11: 431–441.
30. Khan, A.A.; Singh, R.P. (1987) Adsorption thermodynamics of carbofuran on Sn (IV), arsenosilicate in H^+, Na^+ and Ca^{2+} forms. *Colloids Surfaces*, 24: 33–42.